

# Contactless Power and Data Transfer for Multiple Nonlinear Loads

H.-P. Schmidt<sup>\*1</sup>, U. Vogl<sup>2</sup>

<sup>1,2</sup> University of Applied Sciences HAW Amberg -Weiden

<sup>\*</sup>Kaiser –Wilhelm Ring 23, D-92224 Amberg, Germany, h.schmidt@haw-aw.de

**Abstract:** For the design of an inductive power and data transfer electromagnetic calculation are carried out. A transfer system is considered for loads that are distributed across some distances. For example, such loads are adjustable speed drives that are found in factory automation and intra-logistic. Physical properties of the inductive transfer are modeled via COMSOL. Lumped parameters are deduced from magneto static and quasi static calculations. Selected operating conditions are investigated with combined field and network calculations. Field calculations are 2D and 3D and they are carried out for stationary and in the frequency domain. Also heating is modeled at a basic level. Results are compared to experiments that are carried out at a purpose built test stand.

**Keywords:** Contact less power and data transfer, magnetic fields, quasi static EM

## 1. Introduction

The design of a contact less power and data transfer system for industrial applications is studied. We consider the contactless power and data supply of loads such as adjustable speed drives. Such drives are found in automated manufacturing in many industries and they are quite numerous in conveyer systems. Usually such drives consist of a frequency inverter and a motor. In many applications each single drive is connected to the feed cubicle by its own cable. For smaller drives a so called power bus topology may be used were all drives are lined up on a common feed cable. Data links for drive control are realized via a field bus for some dozens of drives.

We focus in this study on small drives with powers not exceeding a few hundred Watts and distances in the range of 10m to 100m. These drives should be supplied by a contactless bus that incorporates the data link. A schematic view of the setup is given in Figure 1. The power feed consists of a controlled H-bridge with adjustable operating frequencies[1]. The feed is inductively coupled to a distributed winding that is run in a

short-circuited mode. The loads are supplied via couplers from this distributed winding. These power couplers consist of ferrite E-cores with I-yoke [2] [3]. For the data transfer we use separate couplers and a separate winding as indicated in Fig. 1.

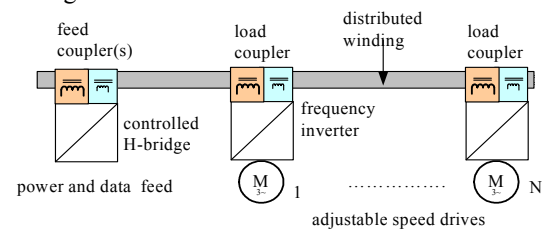


**Figure 1.** Schematic view of inductive power and data transfer.

The feed coupler consists of two windings with  $N_{\text{Feed}}$  turns placed on the shoulders of a ferrite E-core. The I-yoke is separated from the E-core via a small air gap in the range starting under 0.1mm up to 1 mm. The distributed winding is  $N_{\text{dw}}$  turns of a solid or litz wire and the length extends up to 100m. The load couplers are almost the same as the feed coupler as can be seen in Figure 2. They may differ in the depth of E-core and in the number of turns of the winding.

The inductive data transfer design is basically identical to the power transfer system. Here we use smaller E-cores without any yokes. Ferrite and litz wire are suitable for operating frequencies up to 1 MHz. The distributed winding for the data transfer is one single turn made from RF litz wire. As indicated in Figure 2 the data transfer winding is directly attached to one leg of the power winding. Despite this set up interference is still significant, since voltage levels for the power and data link differ by a factor of some thousands. An especially designed OFDM modulation is applied to ensure a reliable communication link for the real time control of frequency inverters. This link uses a bandwidth of app. 600 kHz and is described elsewhere [4].

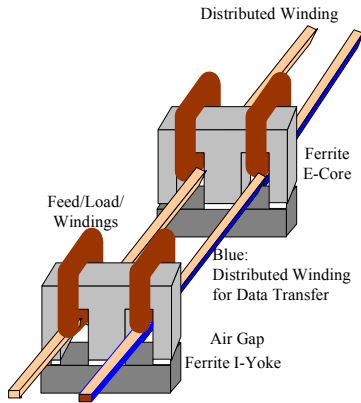


**Figure 2.** Sketch of couplers and their attachment to the distribute winding. The blue face indicates the position of data transfer winding.

## 2. Air Gap Modeling

For the power transfer we need to couple as efficiently as possible. Therefore we look into rather small air gap spacings. These may range from  $10^{-4}$  to  $10^{-2}$  of the core widths. This implies that relevant reluctances are quite sensitive to air gap spacings. To asses the influence the well known magneto static equation for the vector potential with given current densities is solved.

Carrying out 3D studies with a detailed resolution of the air gap yields large numbers of elements with unfavorably size ratios, if the air gap is resolved by at least a few elements with our application. E.g. a 3D mesh which resolves a desired air gap spacing of 0.1mm yields for a single E-Core app.  $15 \times 10^6$  elements. Despite that we applied various meshing domains with adjusted element sizes. Therefore we would like to utilize the thin permittivity layer feature [5].

To asses the influence of the thin layer approximation for our application we carry out a preliminary study. First we use a 2D model for various air gap spacing distances, where the minimum air gap resolution is better than 5 elements. Here a parametric study is conveniently applied with the magnetic field application mode [5]. Secondly, we repeat the calculation with a 3D model applying the thin permittivity layer. The resulting mesh consist now of app.  $5 \cdot 10^5$  elements in contrast to the previous number of

$15 \times 10^6$ . This model can easily be solved in a parametric study for various air gaps.

The comparison of the results is given Figure 3 where the variation of fluxes/reluctances with air gap spacing is shown for 2D, 3D and additionally for a magnetic circuit calculation. On this basis we use the thin layer approximation for our application.

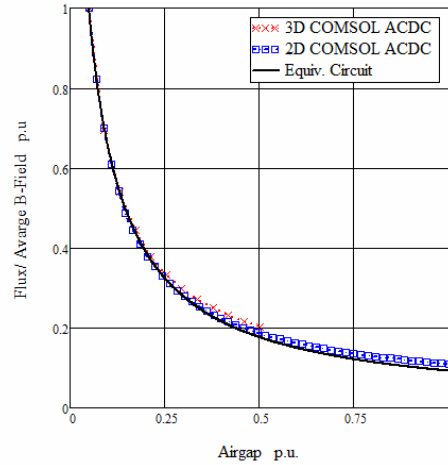


**Figure 3.** Flux/reluctance variation with air gap spacing.

## 3. Lumped Parameter Determination

To study the inductive transfer we use a N-port network for the multi-winding setup. The according equivalent circuit is shown in Figure 4. Assuming identical load couplers yields the equation set 1-3. For system studies and optimizing in regard to compensation capacitances we need to determine the lumped parameters and favorably their geometry/materials dependencies.

$$\underline{U}_F = \underline{Z}_F \cdot \underline{I}_F - j\omega M_{CF} \cdot \underline{I}_{DC} \quad (1)$$

$$0 = \underline{Z}_{DW} \cdot \underline{I}_{DW} + j\omega \cdot M_{DwF} \cdot \underline{I}_F - j\omega \cdot \sum_{j=1}^{N_{load}} M_{DC Li} \cdot \underline{I}_{Li} \quad (2)$$

$$\underline{U}_{Li} = \underline{Z}_{Li} \cdot \underline{I}_{Li} + j\omega \cdot M_{DwLi} \cdot \underline{I}_{DW} + j\omega \cdot \sum_{\substack{j=1, \\ j \neq i}}^{N_{load}} M_{LiLj} \cdot \underline{I}_{Lj} \quad (3)$$

**Equation 1-3.** Legend:  $Z$  denotes the impedances, which include self inductances and joule losses, while  $M$  denotes the mutual coupling inductances. The subscripts F denotes feed, DW the distributed winding and  $L_i$  stands for the  $i$ -th load. For the sake of clarity, stray capacitances, which have to be considered, are not given.

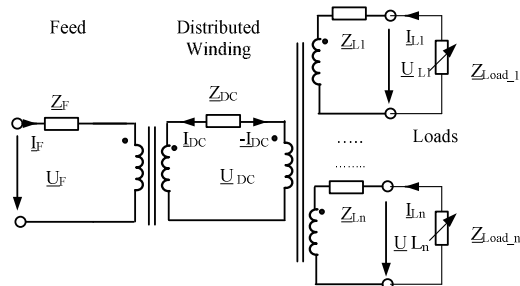


**Figure 4.** Equivalent circuit for the multi-winding model.

Self inductances and mutual couplings were preliminarily determined from the 3D air gap calculations. Self inductances are derived from the total magnetic energy when only one winding is driven by an given current. Mutual inductances are determined via fluxes with according exiting currents. The fluxes are calculated across the appropriate faces and the ratio of flux and current yields mutual inductances when the relevant numbers of turns are taken into account. More detailed studies are carried out utilizing 3D frequency domain calculations coupled to the circuit calculation [5].

We divide the system into a set of three transformers. One consists of the feed and distributed winding, the other of the distributed winding and one load coupler, while the third comprises the load to load coupling. For each of these partial transformers we carry out two no-load calculations where the drive voltage is swapped between both sides of the transformer. The no-load situation is represented by a high resistance value.

The distributed winding is modeled as a multi turn domain coil of the linear type and extends throughout the calculation domain [5]. This domain is app 0.5m x 0.5m x 0.5m. So we model here a short section of the actual winding. This is sufficient for assessing the lumped pa-

rameters and values are easily scaled to the full length of the distributed winding.

The feed and load coupler coils are modeled via two separated multi turn domain coils of the numeric type [5]. They connect to the circuit via one arbitrarily chosen interior boundary. A typical magnetic field for those calculations is given in Figure 5.

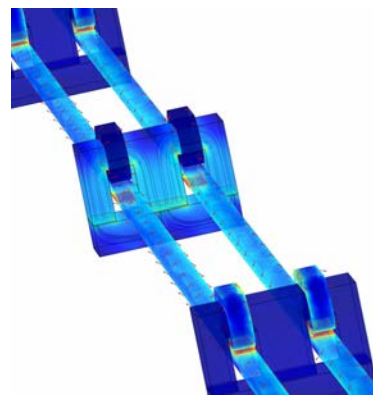


**Figure 5.** Magnetic fields

#### 4. System Study with COMSOL

We model a setup that consists of one feed and two loads which are coupled by the distributed winding. Here the winding extends over 60m. This length is divided into the short section in the FEM calculation domain and a remaining length that is represented by lumped parameters that are part of the circuit calculation. Figure 6 shows how the field calculations are combined with the circuits that are used.

Finally we use the joule heating from the winding to estimate the elevation of the winding and the core temperature with a quite basic model.

#### 5. Experimental setup

We built a test stand with five adjustable speed drives and a distributed winding with 65 m length. Couplers have been built from standard E-Cores, while bobbins have been tailor made. Figure 7 shows the test stand. In the back area are the motors of the adjustable speed drives. The distributed winding is housed in a conduit which meanders along the wooden base plate.

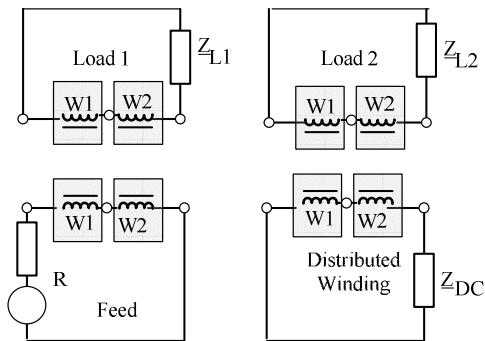


**Figure 6.** Combination of field and circuit calculations. Field calculation are carried out for components that highlighted.

For the measurement of the lumped parameters we use a precision impedance meter to scan the frequency dependencies. Parameters are also measured at realistic power levels. Therefore a frequency synthesizer and a power amplifier are applied as the feeding source instead of the H-bridge. Measurements are taken via a current sensor with a frequency range from DC to 5Mhz and multi channel oscilloscopes for recording. Figure 8 shows the measurement set up.

## 6. Results

The inductances from the COMSOL calculations are validated at low frequencies were the influences of stray capacitances are almost negligible. We find reasonable agreement between measurement and calculation. As an example of the accuracy errors are given for a parameter set at 20 kHz in the table below. For these calculations we find that an appropriate choice between a driving voltage and a driving current important with respect to solution time.

The COMSOL system study that consisted of a feed and two load couplers with all attached to the distributed winding reproduced the voltage transfer ratio from the feed to a load for higher loads within 15%. For the data transfer we determined lumped parameters from low frequency/stationary studies. All of the findings are to be viewed under the prominent air gap dependence of all results. E.g. changes in the air gap as small as 100 $\mu$ m have a significant influence.



**Figure 7.** Test stand with adjustable speed drives and the distributed winding.



**Figure 8.** Measurement set up.

$L_F$	$L_{DW}$	$L_L$	$M_{DW}$	$M_{DWP}$
12%	6%	8%	2%	8%

**Table 1.** Relative errors Key: L self and M mutual inductances. subscript F feed, DW distributed winding and L Load

The temperature elevation was also found to be reasonable despite the rough modeling we used here in contrast to earlier studies [6].

The parameters such as number of turns, voltage levels, geometries and series compensation, which have been collected in this study, have been applied to our test stand. Using the test stand with the controlled H-Bridge we were

able to preliminarily drive and control a few loads.

### **3. Conclusion**

The results from this study have been used to successfully build a first working test stand. Using these calculations was necessary to detail the mutual influences and therefore to adjust the parameters. As expected results are quite sensitive to air gap spacing for our desired small gaps. Therefore the real world application relies on a reproducible air gap to achieve any predicted design performance. The presented work is ongoing and first results have been presented. During the next steps we try to model the transient behavior.

### **8. References**

- [1] Moradewicz A.; Kazmierkowski P. Contactless Energy Transfer System with FPGA Controlled Resonant Converter, IEEE Trans. Industrial Electronics, Vol. 57 No. 9, pp. 3181- 3190, 2010
- [3] Schmidt, H.-P., Gleißner, M.; et. al. : Contact less Power- and Data transfer for Automation. International Forum Mechatronics 2011, Cham, Germany, pp. 491-503, ISBN 978-3-00-0357885-5
- [3] Gleissner, M.; Schmidt, H.-P.; , "Direct and indirect feed-in for inductive power transfer systems with multiple loads," AFRICON, 2011 , vol., no., pp.1-5, 13-15 Sept. 2011
- [4] Schmidt H.-P. , Vogl U. Field bus system with contactless power and data transfer. Proceedings KOMMA 2012, Lemgo, Germany
- [5] COMSOL V4.3 AC/DC User Guide and COMSOL V4.3 Multiphysics User and Reference Guides
- [6] Schmidt H.-P., Efficient Simulation of Thermal and Electrical Behaviour of Industrial Cables, in Recent Advances in Modeling and Simulation, ISBN 978-3-902613-25-7, INTECH, April 2008

### **9. Acknowledgements**

This work is supported by a grant of Bavarian state ministry for sciences and culture.